Microtubular Organization and its Involvement in The Biogenetic Pathways of Plasma Membrane Proteins in Caco-2 Intestinal Epithelial Cells

Thierry Gilbert, André Le Bivic, Andrea Quaroni,* and Enrique Rodriguez-Boulan

Department of Cell Biology and Anatomy, Cornell University Medical College, New York 10021; and *Section of Physiology, Division of Biological Science, Cornell University, Ithaca, New York 14853

Abstract. We characterized the three-dimensional organization of microtubules in the human intestinal epithelial cell line Caco-2 by laser scanning confocal microscopy. Microtubules formed a dense network ~4-μm thick parallel to the cell surface in the apical pole and a loose network 1-μm thick in the basal pole. Between the apical and the basal bundles, microtubules run parallel to the major cell axis, concentrated in the vicinity of the lateral membrane. Colchicine treatment for 4 h depolymerized 99.4% of microtubular tubulin. Metabolic pulse chase, in combination with domain-selective biotinylation, immune and streptavidin precipitation was used to study the role of microtubules in the sorting and targeting of four apical and one basolateral markers. Apical proteins have been recently shown to use both direct and transcytotic (via the basolateral membrane) routes to the apical surface of Caco-2 cells. Colchicine treatment slowed down the transport to the cell surface of apical and basolateral proteins, but the effect on the apical proteins was much more drastic and affected both direct and indirect pathways. The final effect of microtubular disruption on the distribution of apical proteins depended on the degree of steady-state polarization of the individual markers in control cells. Aminopeptidase N (APN) and sucrase-isomaltase (SI), which normally reach a highly polarized distribution (110 and 75 times higher on the apical than on the basolateral side) were still relatively polarized (9 times) after colchicine treatment. The decrease in the polarity of APN and SI was mostly due to an increase in the residual basolateral expression (10% of control total surface expression) since 80% of the newly synthesized APN was still transported, although at a slower rate, to the apical surface in the absence of microtubules. Alkaline phosphatase and dipeptidylpeptidase IV, which normally reach only low levels of apical polarity (four times and six times after 20 h chase, nine times and eight times at steady state) did not polarize at all in the presence of colchicine due to slower delivery to the apical surface and increased residence time in the basolateral surface. Colchicine-treated cells displayed an ectopic localization of microvilli or other apical markers in the basolateral surface and large intracellular vacuoles. Polarized secretion into apical and basolateral media was also affected by microtubular disruption. Thus, an intact microtubular network facilitates apical protein transport to the cell surface of Caco-2 cells via direct and indirect routes; this role appears to be crucial for the final polarity of some apical plasma membrane proteins but only an enhancement factor for others.

EPITHELIAL cells characteristically display two plasma membrane domains, apical and basolateral, with different protein and lipid compositions, separated by tight junctions (for reviews, see references 55, 63). Both the cytoplasmic and submembrane cytoskeletons are also asymmetrically distributed. The polarized organization of epithelial cells accounts for a wide array of vectorial functions involving ion/metabolite transport and protein secretion.

The mechanisms responsible for the establishment and maintenance of epithelial polarity are currently the object of intense study. MDCK cells infected with enveloped RNA viruses that bud from opposite poles (57) have been used to study the intracellular pathways of plasma membrane proteins. Using influenza HA and VSV G protein as model apical and basolateral proteins (58) it was shown that apical and basolateral pathways diverge intracellularly in MDCK cells, at the level of a distal Golgi compartment (40, 45, 52, 53, 56) designated the *trans*-Golgi network (TGN) (24). In the TGN, HA, and G are incorporated into distinct vesicles that are transported to and fuse with, respectively, the apical and the basolateral domains. Recently, distinct post-Golgi vesicle populations carrying either HA or G have been purified from infected, mechanically perforated MDCK cells and shown to display different protein compositions (7, 69); both

apical and basolateral vesicles appear to have affinity for microtubules (67). Development of novel targeting assays based on the use of domain selective biotinylation (37, 61) allowed the extension of the viral studies to endogenous and transfected proteins. Like HA and G, proteins expressed permanently by MDCK cells are sorted intracellularly, presumably in the TGN and are targeted vectorially to the cell surface (35, 38). A similar result was reported for the alpha subunit of Na,K-ATPase (12, 13).

Other epithelial cell types, however, appear to use different strategies to target their surface proteins. In vivo studies with intestinal (26, 39) and liver (5) cells have shown that some apical plasma membrane proteins follow an indirect pathway to the cell surface that includes an intermediate stage at the basolateral domain. Recent studies that applied novel biotin targeting assays to two human intestinal cell lines, SK-CO-15 and Caco-2, showed that some apical proteins were vectorially targeted whereas others used preferentially an indirect (transcytotic) route (34, 36, 42).

An important question is the role played by microtubules in the targeting process. Microtubule-mediated organellar transport is well documented in other systems (11, 27, 28, 30, 41, 66). Although essential for long distance transport of vesicles such as in axonal transport (2), the extent of their involvement in micron-range distances is debated (30). A participation of microtubules in the apical epithelial pathway has been described by several in vivo studies involving destabilizing agents (1, 17, 29, 51). Results of similar studies in MDCK cells are controversial: Rindler et al. reported a missorting of apical HA and no effect on VSV G protein (54) whereas Salas et al. (59) found only minimal effects on the transport of either protein. In Caco 2 cells, the transport of aminopeptidase N (an apical marker) was reported to be affected by nocodazole treatment (21) but only one time point was analyzed and therefore the conclusions reached are necessarily limited.

The availability of precise biochemical targeting assays allows the characterization in detail of the effect of microtubular disrupting agents on the targeting process. Here we describe for the first time the microtubular organization of Caco-2 cells using confocal laser scanning microscopy and use this technique to follow the disassembly of the microtubules under the effect of colchicine. We then characterize the effect of colchicine-induced microtubular disruption on the targeting of four apical and one basolateral plasma membrane proteins in Caco-2 cells. Our results are consistent with a model in which microtubules facilitate the transport of apical proteins to the apical surface via direct and indirect routes and to a lesser extent the transport of basolateral proteins. However, since some of the markers studied have a considerable degree of polarity after microtubular disruption, it is clear that additional mechanisms, such as specific interactions between the vesicle and the target membrane, must play an important role in the sorting process.

Materials and Methods

Reagents

Cell culture reagents were purchased from Gibco Laboratories (Grand Island, NY). Affinity-purified antibodies (rabbit anti-mouse IgG) were purchased from Cappel Laboratories (Westchester, PA). Protein A–Sepharose was from Pharmacia (Uppsala, Sweden), sulfosuccinimidyl 2-(biotinamido) ethyl 1,3-dithiopropionate (s-NHS-SS-biotin) and streptavidin-agarose beads were from Pierce Chemical Co. (Rockford, IL). Rabbit anti-mouse was from Cappel Laboratories, mouse monoclonal anti-alpha-tubulin and fluorescein-conjugated goat anti-mouse were from ICN Biomedicals (Costa Mesa, CA) and Jackson Immuno Research Laboratories, (West Grove, PA). All other reagents were purchased from Sigma Chemical Co. (St. Louis, MO).

Cell Culture and Drug Treatment

The Caco-2 human intestinal cell line was obtained from A. Zweibaum (INSERM U.178, Villejuif, France) and corresponded to late passages (70–80). The cells were maintained in high glucose Dulbecco's modified Eagle's medium (DMEM) supplemented with 10% fetal bovine serum, 1% nonessential amino acids, 1% glutamine, penicillin (50 mU/ml), and streptomycin (50 μg/ml) (normal medium) and cultured in humidified incubators at 37°C with 5% CO_2. For experiments, cells were plated on polycarbonate filters (Transwell; Costar Inc., Cambridge, MA) and grown for 2–3 wk after confluency to ensure optimal differentiation of the cells (49). At that time the transepithelial resistance (TER)[1] was measured with a Millicell ERS system (Millipore Corp., Bedford, MA). After removal of the TER value of the filter itself, the monolayer always exhibited an electrical resistance above 500 ohm.cm^2. Microtubule depolymerization was obtained by the following treatment. After TER measurement, cells were washed twice with ice-cold PBS containing 0.1 mg/ml $CaCl_2$ and 1 mg/ml $MgCl_2$ (PBS/CM), then incubated in cold normal medium containing 10 μM colchicine for 30 min at 4°C and warmed up at 37°C in the presence of the drug for various periods of time, up to 24 h. Control experiments were performed in the presence of 0.04% DMSO. To quantify the extent of microtubular disruption, we extracted tubulin (monomeric and polymeric forms) according to Solomon (64). Samples were processed for SDS-PAGE (10%) and tubulin was revealed by immunoblotting using an alpha-tubulin monoclonal antibody, rabbit anti-mouse IgG and ^{125}I-protein A. The tubulin bands in the fluorograms were analyzed by densitometry.

Antibodies

Monoclonal antibody 525-5-4 against Ag 525 has been previously described (33). Rabbit polyclonal antibodies against human placental alkaline phosphatase were from Accurate Chemical & Scientific Corp. (Westbury, NY). Preparation and characterization of the mouse monoclonal antibodies against sucrase (HSI 9), isomaltase (HSI 14) and aminopeptidase N (HBB2/45) was described previously (6, 36). A monoclonal antibody (DAO7/219) specific for dipeptidylpeptidase IV was similarly prepared using Caco-2 extracts as immunogen and its antigen specificity was determined as previously described (50).

Biochemical Studies

To study the transport of plasma membrane proteins (aminopeptidase [APN], sucrose-isomaltase [SI], alkaline phosphatase [ALP], dipeptidyl-peptidase IV [DPP], antigen 525 [Ag 525]), cells on filters were submitted to pulse-chase protocols similar to those already published (36, 46) using a mix of [^{35}S]-cysteine and [^{35}S]methionine as a label. When the cells were treated with colchicine, the ^{35}S pulse was performed 4 h after the beginning of exposure to the drug at 37°C (i.e. after complete depolymerization of the microtubules) and the times of chase varied from 1 to 20 h in presence of the drug. Filters were then biotinylated from the apical or basolateral side as described (61) and processed for immunoprecipitation and streptavidin precipitation according to Le Bivic et al. (34, 36). Samples were analyzed by SDS-PAGE (31) using 6–12% gradient gels under reducing conditions; the gels were dried and processed for fluorography (15). To study the total protein secretion, aliquots of 25 μl were taken from the apical and basolateral medium at each chase time point and analyzed by SDS-PAGE as described above. To control that colchicine treatment had no effect on the biosynthesis of the markers we followed, the total cellular synthesis of each marker was determined by direct immunoprecipitation of the extracts after pulse-chase

1. *Abbreviations used in this paper*: Ag 525, antigen 525; ALP, alkaline phosphatase; APN, aminopeptidase N; DPP, dipeptidylpeptidase IV; LSCM, laser scanning confocal microscopy; SI, sucrase-isomaltase; TER, transepithelial resistance.

in the presence or absence of colchicine under the same experimental conditions as for cell-surface transport experiments. To study the basolateral to apical transcytosis of APN and DPP, the following protocol was used. After ^{35}S pulse and 60-min chase, cells were labeled with a cleavable biotin (s-NHS-SS-biotin) from the basolateral side for 20 min at 37°C (to avoid any microtubular disruption by a cold treatment). The filters were then incubated for 1–5 h and subjected (or not) to apical reduction with glutathione as previously described (35, 36). Samples were then processed for immunoprecipitation, streptavidin precipitation, and SDS-PAGE and quantitated by densitometry as described above.

Indirect Immunofluorescence and Laser Scanning Confocal Microscopy (LSCM)

Untreated and colchicine-treated (4, 12, and 24 h) cells grown on filters were fixed and processed for microtubular staining according to Drubin (19). Briefly, cells were washed quickly in PBS, fixed 10 min with 0.25% glutaraldehyde in 80 mM Pipes, 5 mM EGTA, 1 mM $MgCl_2$, and 0.5% Triton X-100, pH 6.8, and washed in PBS. Each filter was then cut in four square pieces and incubated with 1 mg/ml $NaBH_4$, freshly prepared in PBS, two times for 5 min. Samples were extensively washed five times in PBS solution containing 1% BSA and 0.1% Tween 20 followed by incubation with the monoclonal antibody diluted 1:1,000 in this buffer and applied on both sides of the filter for 1 h at room temperature. After washing, incubation with FITC-conjugated goat anti-mouse was performed. Finally, samples were washed in PBS and mounted in PBS/glycerol (50:50 [vol/vol]) according to Bacallao (4) with anti-bleaching agent (32). For SI staining, cells were fixed with freshly prepared 2% paraformaldehyde in PBS/CM, followed by a treatment with 50 mM NH_4Cl to quench the free aldehyde groups and then permeabilized with 0.075% saponin. Square pieces of filters were incubated with monoclonal antibodies directed against SI (diluted 1:500 in PBS/CM + saponin + 0.2% gelatin), revealed with FITC-conjugated goat anti-mouse IgG and mounted for LSCM observation.

Specimens were first examined by epifluorescence microscopy (Optiphot, Nikon) using a 100× lens (1.4 NA). LSCM was then performed with a Phoibos 1000 unit attached to the microscope (Sarastro, Ypsilanti, MI). FITC-labeled microtubules were visualized by excitation at 488 nm and emitted light above 515 nm was recorded. The cell monolayer was optically sectioned in horizontal (x-y) planes every 0.2 μm. Series of sections generated through the entire cell height, from the apical to the basal membrane were stored in a Personal Iris workstation (Silicon Graphics, Mountain View, CA) with software provided by Sarastro. Each image was composed of up to 1,024 × 1,024 pixels, with a minimal pixel size of 0.1 × 0.1 μm. Three-dimensional reconstruction of the microtubular network was performed using a Vanis program (Sarastro). Vertical optical section (y-z plane) were also directly obtained with the LSCM. Images generated by the graphics workstation were photographed from the screen using a Nikon Fl camera and a 135-mm objective. Kodak Tmax 100 films were used and processed with Tmax developer.

Electron Microscopy

Control Caco-2 and 6-h colchicine-treated cells grown on filter were washed in cacodylate buffer (0.1 M, pH 7.4) and fixed with 2% glutaraldehyde at 4°C for 1 h in the same buffer. After extensive washing, samples were postfixed in 1% OsO_4, dehydrated in a series of graded ethanol, infiltrated with propylene oxide, and embedded in Epon. Ultrathin sections were cut perpendicular to the filter, and stained with uranyl acetate and lead citrate. Sections were examined with a JEM-100 CXII electron microscope (JEOL) at 80 kV.

Expression of the Results and Statistical Analysis

The films (XAR, Kodak) were preflashed and exposed for 1 d to 1 wk. Two densitometric analyses were carried out for each experiment and the fluorographs were scanned within the limits of linearity as already described (35). For transport experiments, the densitometry values obtained were expressed as a percentage of the amount measured at the time of maximal expression at the cell surface in the absence of colchicine. For transcytosis experiments, the amount of transcytosed protein was expressed as the percentage of the total amount present in the unreduced samples at each time point. Results from two to five independent experiments were averaged and expressed as mean ± SD.

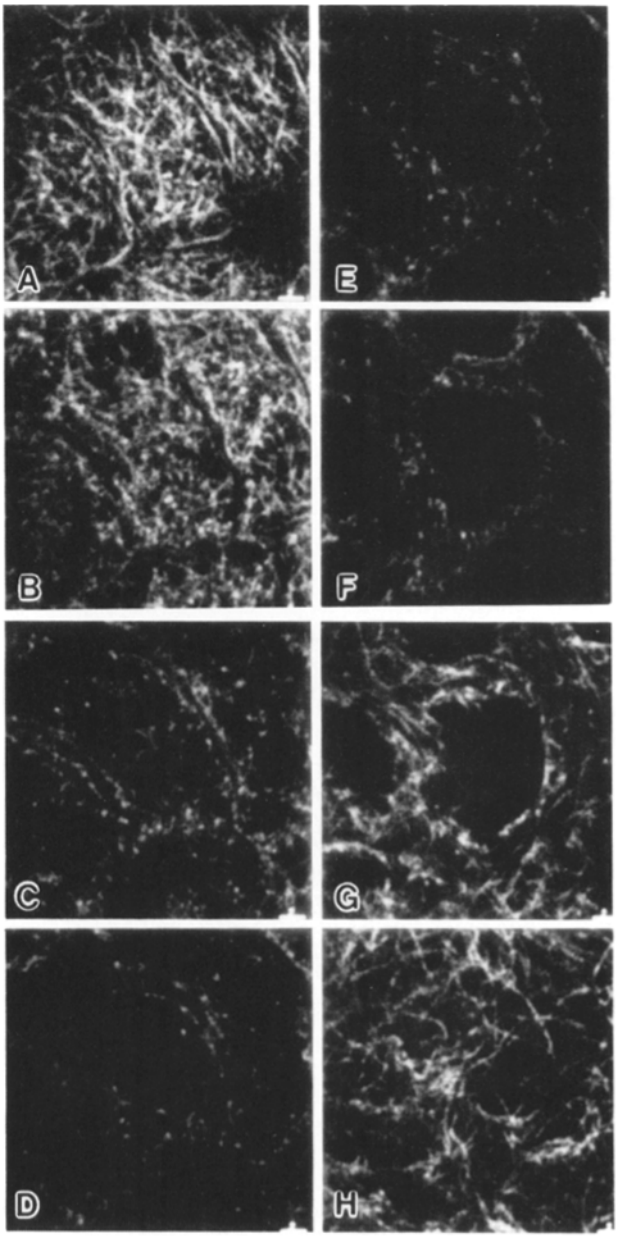

Figure 1. Microtubular organization in Caco-2 cells grown on filters. Monolayers of Caco-2 cells, confluent on polycarbonate filters for at least 2 wk were fixed and processed for indirect immunofluorescence with tubulin antibodies. Horizontal optical planes parallel to the filter were generated by LSCM along an axis perpendicular to the monolayer, from the apex (*A*) to the base (*H*) of the cells. Representative sections are shown from the 82 originally collected. Each image is 256 × 256 pixels and the pixel size is 0.1 μm. The first section is 1.0 μm below the cell surface and the distance between two consecutive images is 2.0 μm. (*A* and *B*) The upper apical region displays a dense network of microtubules running parallel to the cell surface. (*C–F*) The microtubules orient along the major axis of the cell and therefore appear in transverse section as small bright dots; they are concentrated near the lateral plasma membrane forming double images that delineate four cells. The nuclear region is clearly visible in *E–G*. (*G* and *H*) The basal part of the cells shows a sparse microtubular network running parallel to the basal membrane. Bars, 2 μm.

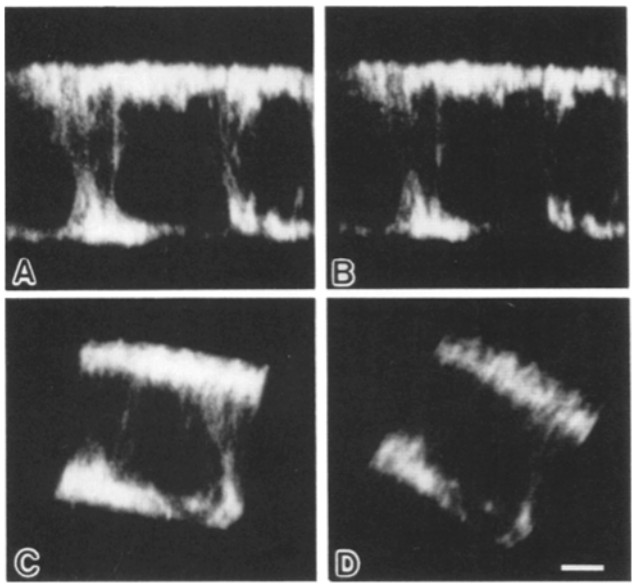

Figure 2. Three-dimensional reconstruction of the microtubular network in polarized Caco-2 monolayers grown on filters. (*A*) Reconstruction of the microtubular network of three neighboring cells. A series of 96 sections, 0.2 μm apart, were collected along the vertical axis of monolayers stained with tubulin antibodies. Three-dimensional image reconstruction was performed with the computer for a prismatic volume (30 pixels or ~3.0 μm thick) selected in the center of the cell. A look-through projection reveals a dense apical tubulin staining of ~4- to 5-μm thick uniformly present below the apical cell surface. (*B*) 5° longitude rotation of image *A*. (*C*) Three-dimensional image reconstruction of the complete volume of one cell, look-through projections. (*D*) 7° latitude rotation of *C*. Some microtubules along the lateral walls can be visualized in their integrity in *C* and *D*. Bar, 5 μm.

Results

Microtubular Organization of Caco-2 Cells

2 wk after plating, human intestinal Caco-2 cells form a fully differentiated monolayer with columnar cells ~20 μm tall, a high expression of apical hydrolases and a highly organized microtubular network. We studied the spacial distribution of the microtubules by LSCM. Series of 80–100 horizontal focal planes of filter-grown fixed monolayers, stained for immunofluorescence with tubulin antibodies, were generated along axes perpendicular to the monolayer. Selected sections of one of such series are shown in Fig. 1. The microtubules present in the subapical region run mostly parallel to the apical cell surface forming a dense network that occupies the top 4 μm of the cell (Fig. 1, *A* and *B*). Deeper down the cell, bundles of microtubules orient longitudinally and therefore project crosssectional images, of bright labeled spots in the peripheral area of the cytoplasm (Fig. 1, *C–F*). Along the later cell borders, microtubules are more concentrated forming double-wall images continuous from the apex to the base of the cells (Fig. 1, *C–F*). Some short longitudinally cut microtubules are present above the nucleus in the Golgi region but do not seem to originate from a single nucleating center (Fig. 1 *C*). In the basal half of the cell, vertically oriented microtubules surround the nucleus (Fig. 1, *E–G*) and, close to the basal membrane, form a flat network parallel to the filter surface, with some microtubules radiating from the nucleus (Fig. 1, *G* and *H*). This basal network is not as dense as the apical one. The digitized images stored in the graphics workstation were used to perform three-dimensional reconstruction. The resulting images, shown in Fig. 2, reveal the complete microtubular organization. Look-through projections combined with latitude or longitude rotations give a clear representation of the large bundles of microtubules surrounding the cells (Fig. 2).

In colchicine-treated cells the microtubular network virtually disappeared. As shown in Fig. 3, treatment for 4 (Fig. 3 *B*), 12, or 24 h (data not shown) results in the complete disappearance of intact microtubules throughout the entire cell height. A faint staining occasionally remained in the most apical region of some cells (Fig. 3 *B*). Examined by LSCM this staining corresponds to very small microtubule fragments (Fig. 3, *C* and *D*, taken at the same depth as Fig. 1, *A* and *B*, respectively). All the other horizontal planes focused deeper into the cell were negative for microtubule staining. We confirmed this result by determining the extent of microtubule disruption by tubulin immunoblot. Quantification of three independent experiments show that in the absence of colchicine 67% of the total cellular tubulin exist in polymeric form and 33% is monomeric. After 4 h of col-

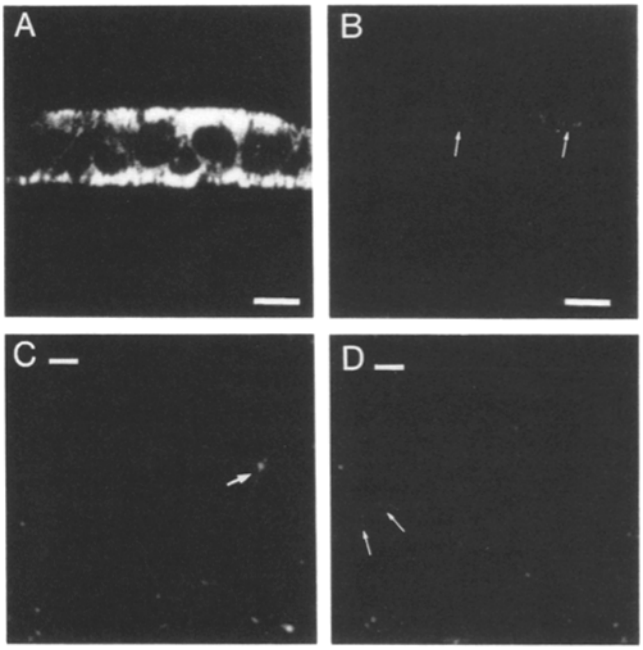

Figure 3. Disassembly of microtubular network induced by colchicine treatment. Monolayers were stained with tubulin antibodies. Vertical sections through the monolayers were obtained by LSCM without three-dimensional reconstruction with an acceptable resolution. Image A and B were taken from fields of 1,024 × 1,024 pixels with a 0.1-μm pixel size. (*A*) Control monolayer. (*B*) Monolayer incubated for 4 h in the presence of colchicine. The microtubular network virtually disappeared. Only a faint tubulin staining was occasionally observed in the upper apical region of the cells (*arrows*). Horizontal sections through the entire cell monolayer was performed as in Fig. 1 to further characterize this staining. (*C* and *D*) Horizontal sections at a depth of 1 and 3 μm from the apical surface of the cells shown in *B*. The faint apical staining of *B* corresponds to small dots (*arrow* in *C*) and very short (*arrows* in *D*) microtubule-like structures. Bars: (*A* and *B*) 10 μm; (*C* and *D*) 2 μm.

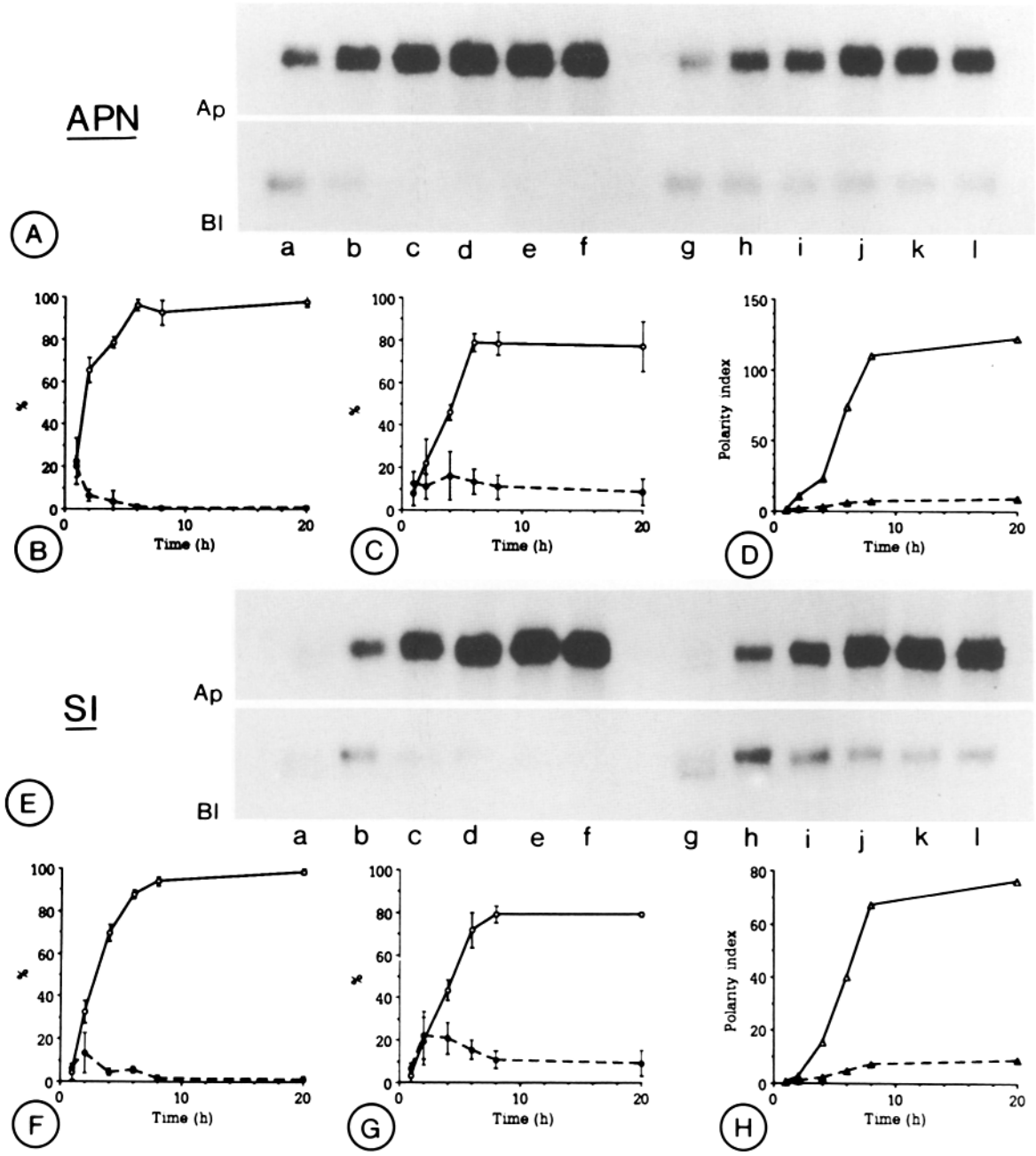

Figure 4. Effect of colchicine on the surface delivery of APN and SI in Caco-2 cells. (*A* and *E*) Confluent Caco-2 monolayers were pulsed for 20 min with [^{35}S]methionine/cysteine and chased for 1 (*a* and *g*), 2 (*b* and *h*), 4 (*c* and *i*), 6 (*d* and *j*), 8 (*e* and *k*), and 20 h (*f* and *l*) in the absence (*a–f*) or presence (*g–l*) of colchicine, added 4 h before the pulse. The monolayers were then biotinylated from the apical (*Ap*) or the basolateral (*Bl*) surfaces, extracted and the fraction of APN (*A*) and SI (*E*) reaching the respective surface determined by immunoprecipitation, streptavidin-precipitation, SDS/6–12% PAGE and fluorography. (*B* and *C*) Densitometric quantification of fluorograph *A*, showing the appearance of APN on apical (*open circles, continuous line*) and basolateral (*solid circles, dotted line*) membrane domain for control (B) and colchicine-treated (C) cells. (*F* and *G*) densitometric quantification of fluorograph E, showing the appearance of SI on apical (*open circles, continuous line*) and basolateral (*solid circles, dotted line*) membrane domain for control (*F*) and colchicine-treated (*G*) cells. Only the mature form of SI was quantified. (*D*) Apical/basolateral APN expression ratio (polarity index) for each time point in control (*continuous line*) or colchicine-treated (*dotted line*) monolayers. (*H*) Apical/basolateral SI expression ratio (polarity index) for each time point in control (*continuous line*) or colchicine-treated (*dotted line*) monolayers.

chicine exposure, almost all tubulin was unassembled (99.4%). The remaining 0.6% of polymeric tubulin may correspond to the punctate staining observed in Fig. 3, *C* and *D*. Colchicine-treated monolayers assembled tight, as determined by TER measurements after 4-, 12-, and 24-h exposure to the drug (TER > 500 ohms·cm^2 at all times).

Effects of Microtubular Disruption on the Transport of Apical Markers

We studied the targeting of four newly synthesized apical markers (SI, APN, ALP, and DPP) to the surface of Caco-2 cells by pulse labeling with [^{35}S]methionine/cysteine fol-

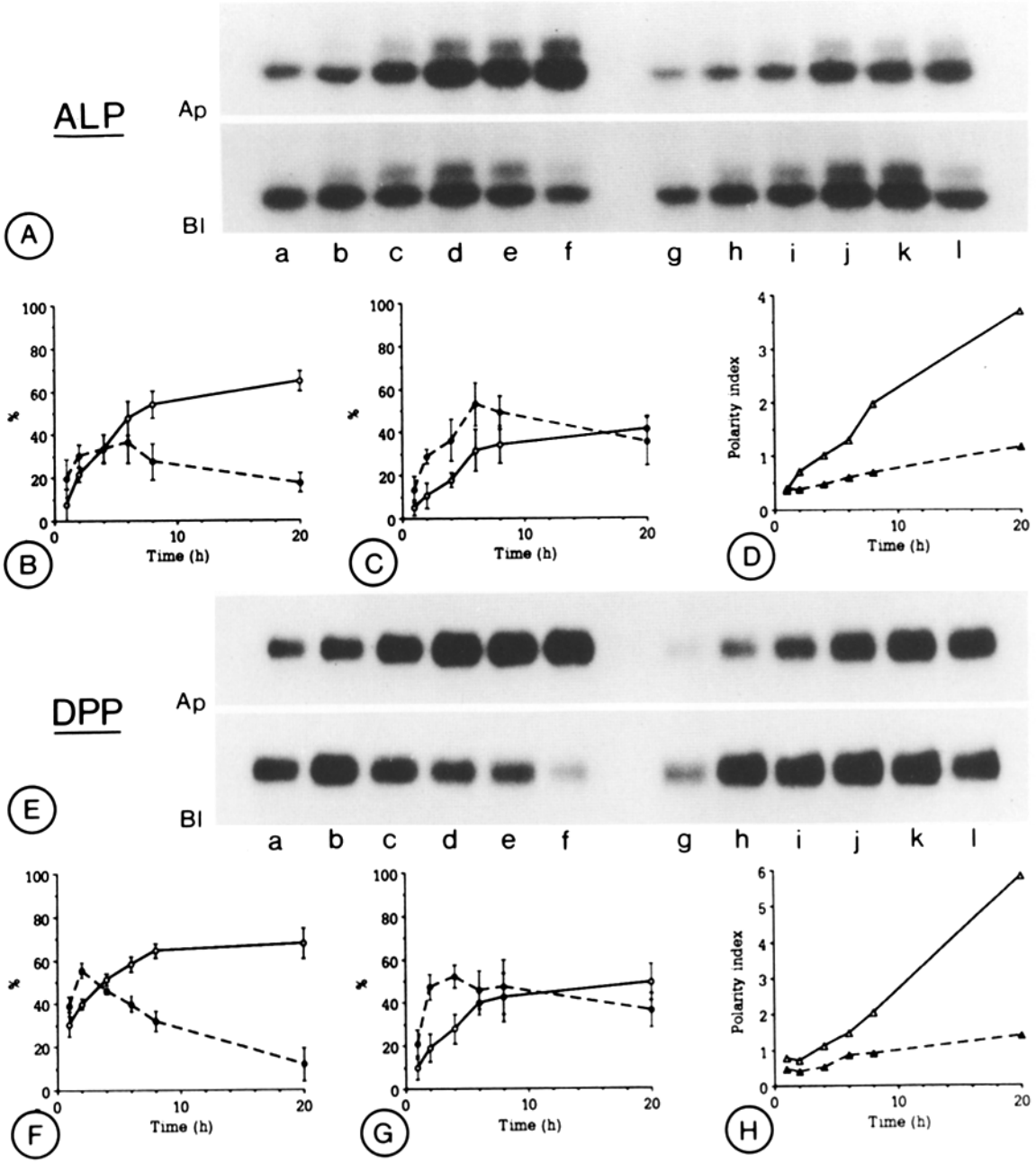

Figure 5. Effect of colchicine on the surface delivery of ALP and DPP in Caco-2 cells. (*A* and *E*) Confluent Caco-2 monolayers were pulsed for 20 min with [^{35}S]methionine/cysteine and chased for 1 (*a* and *g*), 2 (*b* and *h*), 4 (*c* and *i*), 6 (*d* and *j*), 8 (*e* and *k*), and 20 h (*f* and *l*) in the absence (*a–f*) or presence (*g–l*) of colchicine, added 4 h before the pulse. The monolayers were then biotinylated from the apical (*Ap*) or the basolateral (*Bl*) surfaces, extracted and the fraction of ALP (*A*) and DPP (*E*) reaching the respective surface determined by immunoprecipitation, streptavidin-precipitation, SDS/6–12% PAGE and fluorography. (*B* and *C*) Densitometric quantification of fluorograph *A*, showing the appearance of ALP on apical (*open circles*, *continuous line*) and basolateral (*solid circles*, *dotted line*) membrane domain for control (*B*) and colchicine-treated (*C*) cells. Both forms of the ALP doublet were quantified. (*F* and *G*) densitometric quantification of fluorograph *E*, showing the appearance of DPP on apical (*open circles*, *continuous line*) and basolateral (*solid circles*, *dotted line*) membrane domain for control (*F*) and colchicine-treated (*G*) cells. (*D*) Apical/basolateral ALP expression ratio (polarity index) for each time point in control (*continuous line*) or colchicine-treated (*dotted line*) monolayers. (*H*) Apical/basolateral DPP expression ratio (polarity index) for each time point in control (*continuous line*) or colchicine-treated (*dotted line*) monolayers.

lowed by domain-selective biotinylation at different times of chase. Samples were successively precipitated with specific antibodies to the different proteins and the fraction reaching the cell surface determined by precipitation with streptavidin-agarose. Control and colchicine-treated samples were analyzed by SDS-PAGE and the fluorograms quantified by densitometry to determine the profiles of apical and basolateral delivery for each marker. From the curves we estimated the half-times of apical delivery and the polarity index (i.e., apical/basolateral ratio at each time point) for each protein.

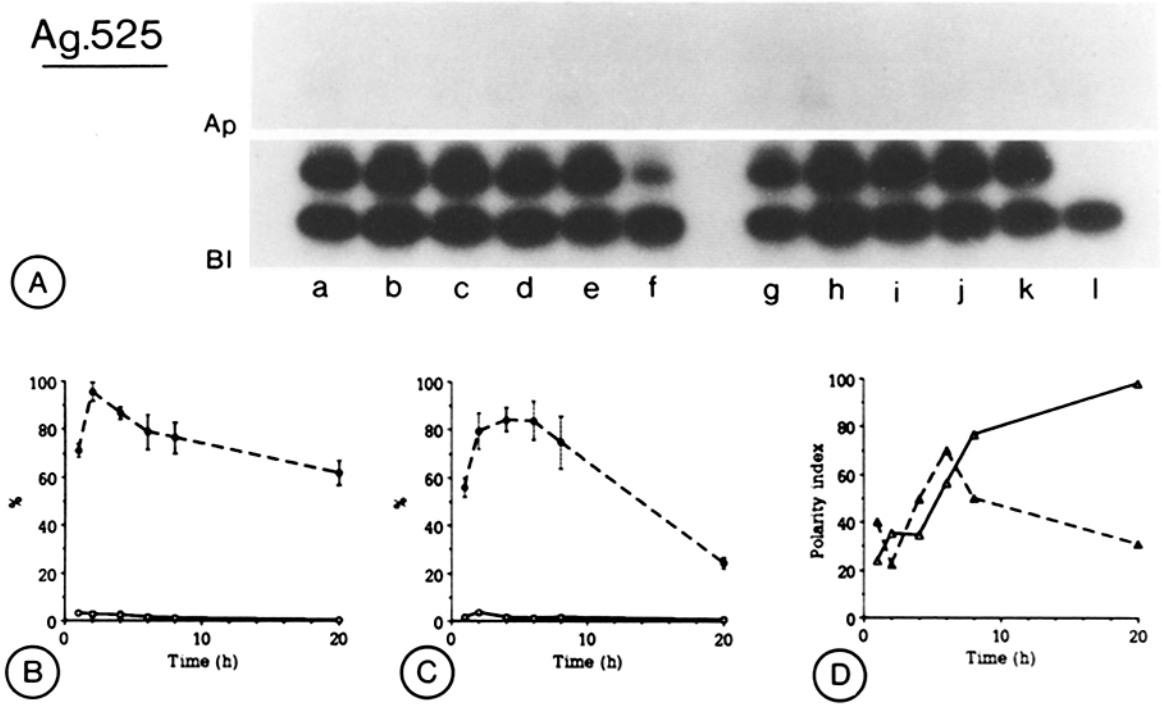

Figure 6. Biogenesis of Ag 525 in Caco-2 cells in the absence or presence of colchicine. The same strategy used for apical markers was applied to characterize the appearance of this marker on both plasma membrane domains. *A* shows the fluorographs: the upper gel represents the apical delivery (*Ap*), the lower one the basolateral appearance (*Bl*); control monolayers are lanes *a–f* and colchicine-treated cells lanes *g–l*, 1-, 2-, 4-, 6-, 8-, and 20-h chase points correspond either to the lanes series *a–f* or *g–l*. (*B* and *C*) Quantification obtained by scanning both bands of Ag 525 for the control and the colchicine group, respectively. The continuous lines correspond to apical appearance and the dotted lines to basolateral expression. (*D*) Polarity index (in this case the ratio basolateral to apical expression) for untreated (*solid line*) or colchicine-treated (*dotted line*) cells.

The levels of synthesis of the markers studied were not affected by colchicine treatment (data not shown). Results for cell-surface expression are reported below individually for each marker.

Aminopeptidase N

The surface appearance of APN at the apical and basolateral domains is shown in the upper half of Fig. 4. Fluorographs of control and treated cells for a typical experiment are shown in *A*; quantitative densitometric data are shown in *B* for control; and in *C* for treated cells. These panels show that initial delivery to the apical surface is markedly reduced by colchicine after 2-h chase (21 vs. 65% for the control) and after 4-h chase (46 vs. 78% for the control). We calculated that in control monolayers, APN was delivered to the apical domain with a half-time of ~1.5 h, whereas in the presence of colchicine the delivery was significantly slowed down ($t_{1/2}$ ~ 3.5 h). Strikingly, despite the total disappearance of the microtubular network, 80% of the APN was correctly targeted to the apical domain after 6 h of chase (Fig. 4 *C*) versus nearly 100% in the control group at the same time (Fig. 4 *B*); these levels remained stable after the overnight chase. The basolateral expression of APN started with a transient peak at around 1 h of chase in control monolayers (20% of the maximal surface expression) (Fig. 4 *B*), consistent with what we previously reported (36). In colchicine-treated cells, basolateral expression of APN appeared to peak later (at ~4 h) and then decreased slowly to ~10% of the maximal control total surface expression (Fig. 4 *C*). Thus, microtubular disassembly slows down apical delivery of APN and disrupts the normal removal from the basolateral surface of the APN pool destined to be transcytosed to the apical surface, at least during the 24-h time frame of the experiments. The apical/basolateral expression ratio was determined for each chase time point (Fig. 4 *D*). The resulting "polarity index" of APN increased with time and after 8 h reached a value of 110 in control monolayers, close to the value that we previously observed at steady state (36), confirming the high degree of polarization reached by this glycoprotein. In colchicine-treated cells, APN surface expression reached a polarity index of ~9 after overnight chase, which still reflects a considerable degree of polarity. At early chase times (i.e., 2 h), control monolayers expressed 10 times more APN on the apical than on the basolateral side, compared with only 2 times in colchicine-treated cells, in complete accordance with previously published data (21).

Sucrase-isomaltase

The pattern of surface expression of newly synthesized SI (Fig. 4, *bottom*) exhibited similarities to APNs. As shown in Fig. 4, *E* and *G*, the initial apical delivery is slightly retarded in colchicine-treated cells and is lower at 4 h of chase (44 vs. 70% in controls). SI appeared on the apical domain with a half-time of ~2.5 h and displayed a basolateral peak after 2-h chase (representing ~13% of the total maximal surface expression), which decreased slowly with time (Fig. 4, *E* and *F*). In monolayers treated with colchicine the transport of SI to apical surface occurred with a half-time of

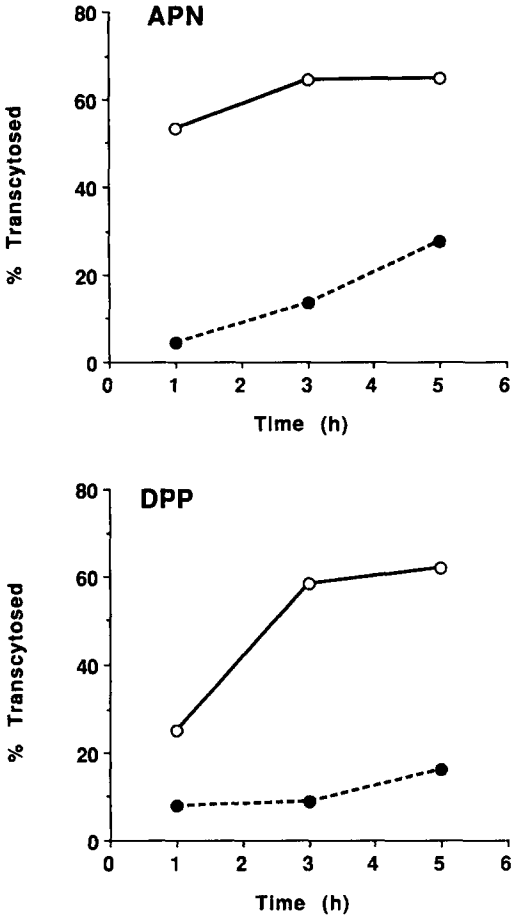

Figure 7. Effect of colchicine on basolateral to apical transcytosis of APN and DPP. Confluent control (*open circles*) and colchicine-treated (*solid circles*) Caco-2 monolayers were pulse labeled, chased for 60 min, and basolaterally biotinylated for 20 min at 37°C. The cells were then incubated at 37°C for the indicated intervals of time and subsequently reduced (or not) from the apical side with glutathione. The amount of immunoprecipitable biotinylated APN and DPP was then determined and quantified. The results are expressed as the percentages of the basolaterally biotinylated pool of each peptidase that reach the apical surface at each time point, for control and colchicine-treated cells.

~4 h and reached almost 80% of control values after 8-h chase (Fig. 4 *G*) compared with ~95% in control monolayers. At the 2-h chase time, the basolateral and apical expression levels of SI were similar (22 and 19% of total surface control expression, respectively). After 2-h chase, the basolateral level of SI decreased to ~1.5% in control monolayers at 8- or 20-h chase times (Fig. 4 *F*) but only to ~10% in colchicine-treated cells (Fig. 4 *G*), as observed for APN (Fig. 4 *C*). With the incomplete removal of basolateral pool, the polarity index reached only a value of 9 for the treated cells instead of ~70 in control monolayers (Fig. 4 *H*); the control value is similar to the one we previously reported for the steady-state distribution of the enzyme (36).

Alkaline Phosphatase

The pattern of surface expression of ALP is shown in Fig. 5 (*top*). In control monolayers, ALP was delivered to the apical surface with an estimated half-time of ~4 h (Fig. 5, *A* and *B*); a broad basolateral ALP peak (up to 36% of the maximal total surface expression) was present during an 8-h chase period and 17.5% was still detected in this membrane after an overnight chase (Fig. 5, *A* and *B*). The 18% loss of basolaterally expressed ALP after 6-h chase in control cells was exactly compensated by a 17% increase in its apical appearance. These results suggest that, although ALP is transcytosed very slowly from the basal to the apical surface (36), a sizeable fraction may reach the apical surface after insertion in the basolateral membrane. In colchicine-treated cells (Fig. 5 *C*) the apical delivery curve was flattened, consistent with a transport slow-down induced by microtubule depolymerization. The amount of ALP detected on the basolateral side was actually higher than on the apical side during most of the chase, decreasing to levels similar to the apical side by 20 h. 18% of the newly synthesized ALP disappeared from the basolateral plasma membrane between 6 and 20 h of chase but only 10% appeared on the apical surface, suggesting that part of this marker was degraded or sequestered intracellularly. Accordingly, the polarity index raised very slowly to a value of ~4 in controls but remained under 1 at all times in colchicine-treated cells (Fig. 5 *D*). Thus, ALP reaches only a modest level of polarization (polarity index of 4 under our chase conditions, 9 at steady state [36]), which appears to be completely abolished by microtubule depolymerization.

Dipeptidylpeptidase IV

The sorting of newly synthesized DPP is represented in the bottom half of Fig. 5. The steady-state distribution of this enzyme under our culture conditions, determined by a biotin polarity assay (36), was preferentially apical by a ratio of 8 to 1. There were many similarities between the surface targeting of ALP and DPP. In controls, DPP appeared on the apical surface with a half-time of ~1.5 h (Fig. 5, *E* and *F*); a large fraction was initially delivered to the basolateral surface (56% of the total maximal surface expression at 2 h of chase) and then regularly decreased with time to represent 32% at 8 h and only 11% after 20 h of chase. The decrease in basolateral expression between 8 and 20 h was not accompanied by an increase in the apical pool, which remained constant at 65–68% in the same period. This indicates that a large pool of DPP (~20% of the newly synthesized protein) remained intracellular with a fraction of it probably targeted for lysosomal degradation (44). In colchicine-treated cells, however, the basolateral peak of ALP was much broader than in control cells with 36% of the maximal surface expression still expressed in this surface after a 20-h chase (Fig. 5 *G*). These results are consistent with a decreased ability to remove basolateral DPP and transcytose it to the apical surface in the absence of microtubules. As for ALP, the polarity index of DPP was small (~6 after overnight chase) and decreased to below 1 in colchicine-treated cells (Fig. 5 *H*).

Effects of Colchicine Treatment on the Transport of a Basolateral Marker

We followed the appearance of Ag 525 using the same approach as described for apical markers (Fig. 6). Ag 525 was previously well characterized (33) and is almost exclusively present on the basolateral domain of Caco-2 cells and other human colon intestinal cell lines. As shown on Fig. 6, *A* and

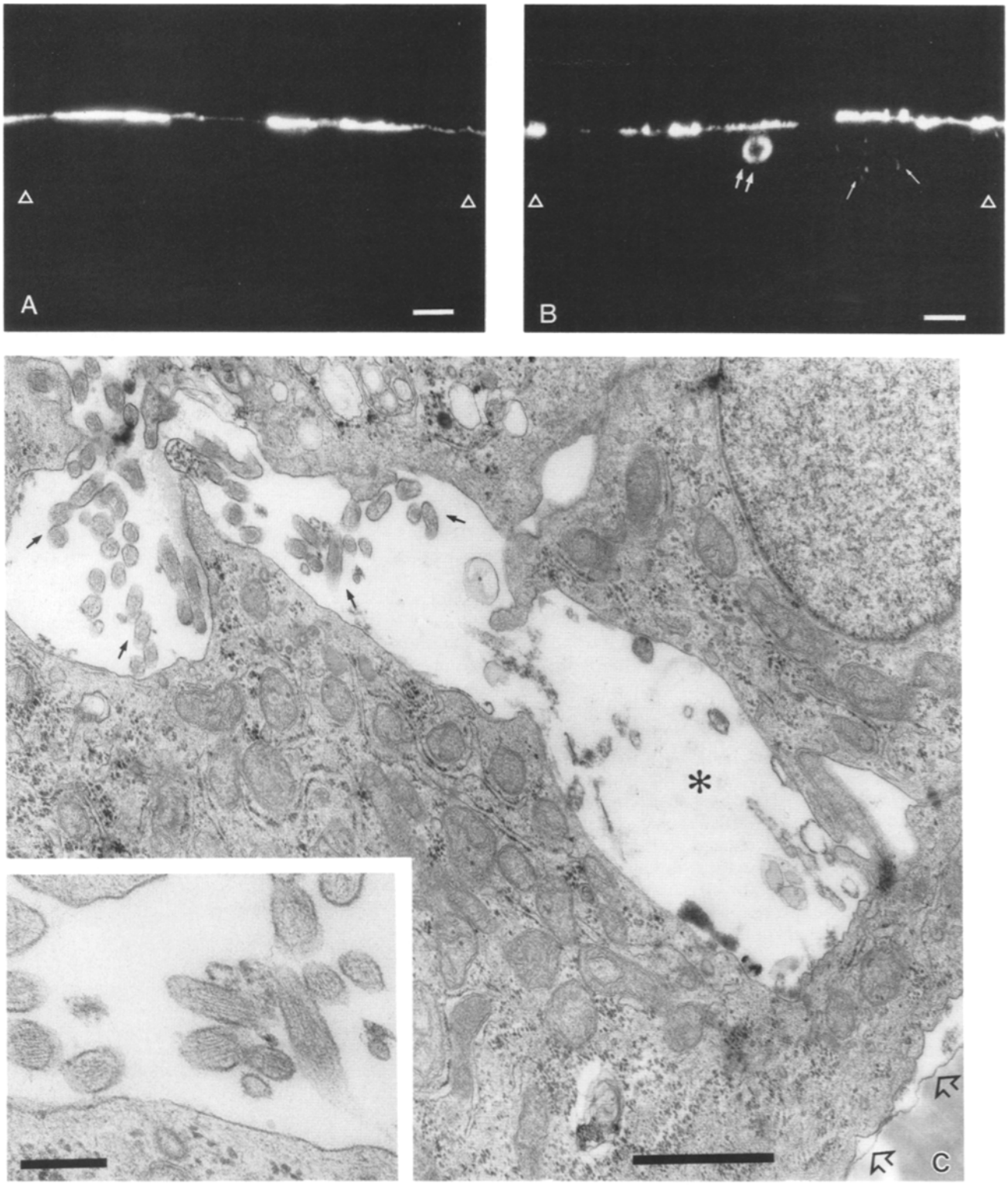

Figure 8. Ectopic expression of apical markers in intracellular vacuoles and basolateral membranes. (*A* and *B*) Vertical LSCM sections of Caco-2 monolayers grown on filters processed for indirect immunofluorescence with SI antibodies. (*A*) Control and (*B*) colchicine-treated (6 h) cells were fixed with freshly prepared 2% paraformaldehyde in PBS/CM, permeabilized with 0.075% saponin and exposed to monoclonal antibodies directed against SI, subsequently revealed by FITC-conjugated goat anti-mouse IgG and mounted for LSCM observation. A large intracellular vacuolar component containing SI is seen after colchicine treatment (*double arrows*, *B*). *B* also shows some staining of the basolateral plasma membrane (*single arrows*). Open triangles indicate the position of the cell-filter interface. (*C*) Electron micrograph of filter-grown Caco-2 monolayers treated with colchicine for 6 h. Note the presence of microvilli-like structures (*arrows*) protruding into the intercellular space (*) from the lateral membrane. Open arrows indicate the interface between filter and basal plasma membrane. (*Inset*) Higher magnification of a microvilli-rich area of the lateral membrane. Note the presence of filament bundles in the microvilli. Bars: (*A* and *B*) 10 μm; (*C*) 1 μm; (*inset*) 0.2 μm.

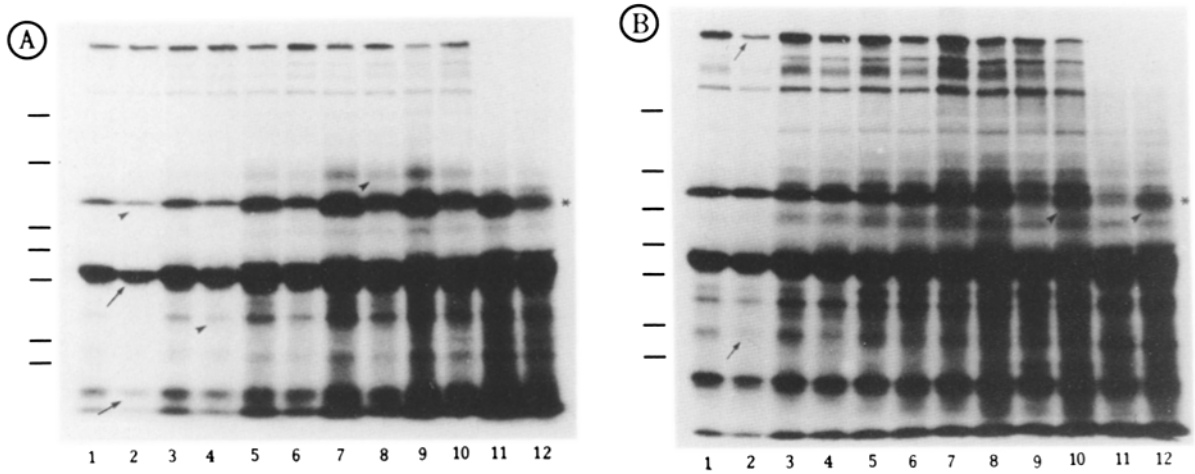

Figure 9. Protein secretion in Caco-2 cells in the absence or presence of colchicine. Caco-2 monolayers were subjected to a pulse-chase protocol as described in Figs. 4–6. At different times of chase, aliquots of apical and basolateral medium were collected and analyzed by SDS/6–12% PAGE followed by fluorography. (*A* and *B*) Apical and basolateral secretion, respectively. Control (*even numbers*) and colchicine (*odd numbers*) lanes are shown for each chase time point, i.e., 1 (lanes *1* and *2*), 2 (lanes *3* and *4*), 4 (lanes *5* and *6*), 6 (lanes *7* and *8*), 8 (lanes *9* and *10*), and 20 h (lanes *11* and *12*). Arrows, arrowheads, and asterisks refer to specific comments as stated in Results. Molecular mass standards (180, 116, 84, 58, 48, 36, and 26 kD) are represented by bars (*top to bottom*) to the left of each gel.

B, the basolateral delivery is extremely fast ($t_{1/2}$ ~40 min) (extrapolation of the curve to the initial point) and efficient (96% of the total maximal surface expression). After the initial delivery stabilized, a decrease in surface expression was observed, which occurred in two phases: a rapid one and a slow one. These kinetics are consistent with the possibility that Ag 525 be a recycling receptor (10, 62). Surprisingly, both the transport and surface stability of newly synthesized Ag 525 were partially sensitive to colchicine (Fig. 6 *C*). In drug-treated cells, the basolateral expression of Ag 525 was significantly lower than control at 1 and 2 h of chase and remained low after 20-h chase (<25 vs. 62% in control monolayers). This behavior in the presence of colchicine suggests that an endocytosed pool of Ag 525 is unable to be recycled to the basolateral domain and remains intracellular or is degraded. In colchicine-treated cells as in untreated cells, the maximal apical cell surface expression represented <3% of the total cell surface expression. Examination of the polarity index (which represents in this case the basolateral/ apical ratio) in Fig. 6 *D* clearly shows a decrease after 6 h whereas it increases in the untreated cells. In microtubule-disrupted cells the polarity index reached by Ag 525 is three times lower than in control cells but a substantial level of polarity persists (about 30 times).

Effect of Microtubular Disruption on Transcytosis of APN and DPP

We examined the effects of colchicine on the basolateral to apical transcytosis of two apical markers, APN and DPP. Our previously described transcytosis assay (36) was modified by biotinylating the basolateral plasma membrane for 20 min at 37°C instead of at 4°C, to avoid cold-induced microtubular disruption (3), which might slow down transcytotic abilities of control cells. Control and colchicine-treated monolayers were pulsed with [^{35}S]methionine/cysteine for 20 min and chased for 60 min before biotinylation from the basolateral side. (As shown in Figs. 4 and 5, the percents of newly synthesized peptidase detected on the basolateral plasma membrane domain at about this time [1-h chase] are ~20% for total APN and 39% for DPP. In colchicine-treated cells, these values dropped to 13% for APN and 21% for DPP.) The filters were then incubated for various times with the chase medium and then reduced with glutathione from the apical side. Fig. 7 shows the effect of colchicine on the transcytosis of APN and DPP to the apical surface. In control cells, 65% of basolaterally biotinylated APN was transcytosed in 3 h with no additional increase at 5 h; the half-time of transcytosis appeared to be <1 h for APN. For DPP, only 25% was transcytosed in 1 h (vs. 53% for APN) and at 3 and 5 h ~60% appeared on the apical surface. Failure to reach 100% transcytosis was observed consistently and may be attributed to incomplete reduction of apical antigen by glutathione (36). Colchicine-treated cells showed a dramatic decrease in transcytosis. For APN, only 5% was transcytosed in 1 h and 13% in 3 h, whereas by 5 h the levels had raised to ~30%. For DPP, only background levels of transcytosis were observed for the first 3 h, with a slight increase in the amount transcytosed (to ~14%) by 5 h.

Ectopic Expression of Apical Markers in Colchicine-treated Cells

Upon examination of the total surface expression of apical markers in colchicine-treated cells, we noticed that a substantial fraction of these newly synthesized proteins (at least ~10%) never reached the apical cell surface after the overnight chase. We observed by indirect immunofluorescence and LSCM that, as previously reported in native intestinal epithelia of rats injected with colchicine (1), a fraction of the apical markers is found in large intracellular vacuoles and in the basolateral surface as shown on Fig. 8 *B* for sucrase-isomaltase. Electron microscopy examination revealed that this basolateral expression may be accounted for by the appearance of ectopic microvilli along the lateral plasma membrane (Fig. 8 *C*), an event previously described in intestinal epithelial cells of colchicine-treated rats (1, 48). Microvilli were also observed in large intracellular vacuoles such as

the one shown on Fig. 8 *B* (Gilbert, T., and E. Rodriguez-Boulan. 1990. *J. Cell Biol.* 111 [No. 5, Pt. 2]:328a[Abstr.]).

Effects of Microtubular Depolymerization on Protein Secretion

We studied the total pattern of proteins metabolically labeled during the short pulse experiment and secreted either into the apical or basolateral media by analyzing by SDS-PAGE aliquots taken at each chase time point. The corresponding fluorographs are shown on Fig. 9. No qualitative differences appeared between the control and the colchicine groups for proteins in the apical or basolateral media; however, densitometric analysis revealed quantitative differences in apical and basolateral patterns. The secretion of some apical proteins was inhibited by colchicine; this inhibition disappeared at later time points, consistent with a delay in secretion (see *arrow*, Fig. 9 *A*). Other proteins suffered a more irreversible inhibition (*arrowheads*, Fig. 9 *A*). Fig. 9 *B* also indicates that the secretion of some basolateral proteins was sensitive to colchicine exposure (particularly evident after 1 h of chase). 75% inhibition was observed (quantification not shown) for some high or low molecular weight proteins (see *arrow*, Fig. 9 *B*). On the other hand, after an overnight chase, some proteins still present a threefold increase in basolateral expression as compared to the untreated cells (see *arrowheads*, Fig. 9 *B*). At that time of chase these proteins (Fig. 9 *B*, *asterisk*) seem to have a nonpolarized secretion (50/50) versus a preferential apical secretion under normal conditions (80/20).

Discussion

The human adenocarcinoma cell line Caco-2 has recently received increased attention as a model for the study of the biogenesis of surface polarity in intestinal epithelial cells. This cell line is now well characterized ultrastructurally and biochemically (49) and studies have recently been reported on membrane traffic processes in these cells that may depend on microtubules (36, 42, 44). However, the microtubular organization of Caco-2 epithelial cells has not been studied in detail. In this report, we use LSCM to study the three-dimensional distribution of microtubules in well-polarized, filter-grown Caco-2 cells. Our results indicate that microtubules exhibit a general longitudinal orientation parallel to the lateral cell walls, similar to that observed in differentiated small intestine enterocytes (1, 29). In the neighborhood of each cellular pole, however, microtubules formed a dense microtubular network under the apical surface and a sparse one close to the basal membrane. Similar microtubular bundles parallel to the apical and the basolateral surfaces were recently described in confluent monolayers of MDCK cells (3); this specialized organization may thus be a common feature of fully polarized epithelial cells. The longitudinally oriented microtubules likely have their plus ends in the basal region because colchicine treatment, known to alter more efficiently the plus end than the minus end (70), effected depolymerization more rapidly in the basal area (data not shown). The most effective depolymerization protocol was a combination of 30 min in the cold in the presence of colchicine followed by colchicine at 37°C, in agreement with previous observations (3). This treatment led to a complete disappearance of intact microtubules (as confirmed by the practically complete disappearance of polymerized tubulin), which persisted for at least the 24-h period used in all subsequent experiments. This is expected from previous reports that indicate that colchicine treatment is quite irreversible (20, 22).

In native intestinal epithelia, microtubules have been shown to traverse the terminal web (25, 60), with many ending in anchorage sites at the apical plasma membrane (the latter particularly observed in *Drosophila* [65]). The faint punctate staining of tubulin we observed in the most apical region of colchicine-treated cells may correspond to such sites. Alternatively this staining pattern may represent nucleating centers of microtubules running parallel to the apical surface which were protected by microtubule-associated proteins, as suggested by Bacallao et al. (3) for MDCK cells. Nevertheless, it is clear that no intact microtubules remained in Caco-2 cells subjected to the cold colchicine protocol (only 0.6% polymeric tubulin, as determined by immunoblot). This point needed to be stringently assessed as a preliminary step to our studies on the targeting of Caco-2 plasma membrane proteins.

A disruptive effect of microtubule-depolymerizing drugs, mostly colchicine, on protein transport in enterocytes has been previously described (8, 17, 47, 51). More recently, Eilers et al. reported that nocodazole-treatment in Caco-2 cells resulted in partial missorting to the basolateral surface of an apical protein (21). At the time when those studies were performed, the normal pathways of plasma membrane proteins in Caco-2 cells had not been studied. The recent characterization of direct and indirect pathways in liver (5), MDCK (35), and Caco-2 cell lines (36, 42) prompted us to evaluate the microtubular involvement in the biogenesis of Caco-2 plasma membrane proteins. To this end, we used novel targeting assays based on a domain-selective biotinylation procedure introduced by our laboratory (37, 61).

Our experiments show that the final effect of microtubular disruption depends to a large extent on the protein under study. Our results confirm previous evidence indicating that the targeting of apical proteins is perturbed more intensely than the targeting of basolateral proteins (21). However, some effects were clearly evident on the transport and final distribution of Ag 525, the basolateral marker studied here. The half-time of basal delivery was increased from 30 to 60 min and the final polarity of this antigen was reduced threefold. A 30-fold level of polarization remained, suggesting that microtubules facilitate the polarization of Ag 525 but are only a relatively minor factor.

Apical proteins that normally reach highly polarized distributions, such as APN and SI (polarity indexes close to 100), retained a considerable degree of asymmetry after microtubule depolymerization (about ninefold). The appearance on the apical domain of newly synthesized APN and SI was considerably slowed down by colchicine treatment, with 80% of the newly synthesized protein reaching the apical surface after 6–8 h of chase (Fig. 4, *C* and *G*), instead of after ~2 h as observed for control (untreated) cells. Since it has been shown that about half of the newly synthesized APN reaches the apical surface via a direct route and half via an indirect (basolateral) route (43), it was necessary to establish which one of these pathways were affected by colchicine. Because only 20% of APN had arrived at the apical surface after 2 h of chase in the presence of colchicine, it is

clear that microtubule disruption affected the direct pathway. To study the effect of colchicine on the indirect pathway, we measured the basal to apical transcytosis of APN in the presence of the drug. These experiments showed a large inhibition in cells with microtubular disruption, which was partially overcome over a period of 5 h (90% inhibition after 1 h of chase vs. 50% inhibition after 5 h of chase). Thus, our results indicate that microtubules facilitate transport of APN via both direct and indirect routes; however the requirement for microtubules is not absolute since a large amount of APN (~80%) eventually reaches the apical surface.

The transcytosis experiments revealed control rates of transcytosis of APN faster than reported previously by our laboratory (36) and by Matter et al. (42), using similar biotin targeting assays. Whereas in those reports maximal transcytosis of APN was observed only after 3 h of chase, the experiments described in this paper indicate that transcytosis of the basolaterally biotinylated pool of APN was practically complete after one hour (82% of the maximal value, shown in Fig. 7 and observed in two independent experiments). We believe that the transcytotic rate of APN reported here reflects the actual rate more closely than previously reported for two reasons. (*a*) The transcytosis assay used here does not include a preincubation step at 4°C whereas the two previous reports mentioned above included a low temperature preincubation lasting for at least 90 min. This low temperature treatment immediately before the assay may in itself depolymerize a large fraction of microtubules and therefore considerably slow down transcytosis. (*b*) The fast transcytotic rate observed in this report is in closer agreement with the results of targeting assays reported by both laboratories (see Fig. 4 *B* of this paper, Fig. 4 of reference 36 and Fig. 5 of reference 42), which (as mentioned above) indicate that delivery of APN to the apical surface is practically complete in 2–3 h.

Interestingly, the basolateral expression of APN and SI, usually transient and decreasing to ~1% in control cells, was larger and more prolonged in colchicine-treated cells, stabilizing after an overnight chase at ~10% of the total maximal surface expression. The appearance of a stable pool of APN on the basolateral surface may reflect the formation of apical-like microvilli in this membrane in colchicine-treated cells. Several laboratories have described this phenomenon in the intestinal epithelium of colchicine-treated rats (1, 48). We observed the presence of microvilli in both the basolateral surface and in intracellular vacuoles of colchicine-treated Caco-2 cells (Fig. 7 *C* and Gilbert, T., unpublished data). Unlike basal microvilli in native epithelial cells (1), basolateral microvilli induced by colchicine in Caco-2 cells seem to be relatively stable during the time of the experiment. These misplaced pieces of apical membrane remain segregated from the remaining basolateral membrane, instead of intermixing with it (the microvilli were usually present in clusters).

Since endocytosis from the apical surface is much less efficient than from the basal surface (36, 44), basolateral microvilli provide a relatively stable population of SI and APN that cannot be removed during the time frame of the experiments described here. Because the drop in polarity of SI and APN mainly depends on the increase in the basolateral expression of these enzymes (from 1 to 10%, probably trapped in the ectopic microvilli), it is clear that the targeting of the bulk (80%) of these two enzymes is not greatly affected by the colchicine treatment. This suggests that additional mechanisms besides microtubules contribute to the generation of polarity of Caco-2 cells with the main role of microtubules being the facilitation of direct and transcytotic vesicle delivery to the apical surface. Through this facilitation, microtubules contribute to a more stringent polarization of apical surface markers.

ALP and DPP have a very different sorting pattern from APN and SI but their biogenesis appears to be similarly affected by microtubular disruption. A larger fraction of these proteins is expressed on the basolateral surface at steady state (~15%), apparently because of both a very large initial delivery to the basal surface (at least 60% for DPP, see Fig. 5 *F*) and slow transcytosis (36, 42). The control targeting polarity ratios after 20 h chase were ~4 and ~6 for ALP and DPP, respectively (~9 and ~8 at steady state), and were reduced to <1 in colchicine-treated cells. Direct measurement of DPP transcytosis from the basolateral to the apical side indicated a slower rate than for APN, as previously reported (42). However, the transcytotic rate observed here was, as described for APN, greater than previously reported, most likely because of artifactual disruption of microtubules introduced by cold preincubation in the previous report (42).

Unlike APN and SI, ALP and DPP were unable to polarize in the absence of microtubules. The apical delivery curves were flattened and the basolateral residence times greatly increased for both enzymes (compare Fig. 5, *C* and *G* with Fig. 5, *B* and *F*). This may be a consequence of the slower transcytosis of these proteins in control cells, which become even slower in the absence of microtubules.

The signals for transcytosis have recently been elucidated for one protein. Recent work by Mostov's laboratory has defined sequences in the cytoplasmic domain of Poly-Ig receptor that mediate removal from a basolateral recycling pathway and incorporation into vesicles destined for apical transcytosis (14). Since in the endocytic pathway, late but not early endosomal fusions appear to require microtubules (9), it is likely that microtubules facilitate the incorporation of basolateral pools of apical proteins from recycling endosomes into transcytotic vesicles. We hypothesize that if this is an efficient process (e.g., APN and SI) microtubule facilitation may simply act as an enhancer; if this is an inefficient process (e.g., DPP and ALP) microtubule facilitation becomes a crucial factor in the polarization of the protein. Thus, although the general effects of microtubule disruption on the biogenesis of DPP and ALP are the same as for the better polarized SI and APN, the consequences for the polarized distribution of these two normally poorly polarized proteins are much greater, since their asymmetric distribution is lost. Recent progress in the purification of transport vesicles (69) should allow stringent testing of this hypothesis.

As discussed above, only 80% of newly synthesized APN and SI reach the apical surface in the presence of colchicine, with ~10% remaining stably on the basolateral surface, apparently in ectopic microvilli (Fig. 7 *C*). The remaining 10% of SI and APN that fails to reach the apical surface is probably stored in large intracellular vacuoles such as shown in Fig. 7 *B* or in small post-Golgi vesicles. In the intestinal epithelium of colchicine-treated rats, large "brush-border vacuoles" were observed that appeared to originate from endocy-

tosis of basolateral microvilli (1), whereas in Caco-2 cells they appear to be produced de novo in the cytoplasm (Gilbert, T., and E. Rodriguez-Boulan, manuscript in preparation). The appearance of intracellular vacuoles with inwardly facing microvilli was described as a major morphological characteristic of a familial enteropathy called Davidson's disease or microvillus inclusions disease (16, 18). It is remarkable that the Caco-2 cell line exhibits similar characteristics and behavior than small intestine enterocytes and this turns them into a potential in vitro model for study of this enteropathy. Furthermore, similar vacuoles have also been described in MDCK cells cultured in the absence of cell–cell contacts (68).

In summary, our results indicate that microtubules play a facilitating role in the targeting of plasma membrane proteins to the cell surface. This facilitation is more important for apical protein targeting, although we also describe here microtubular involvement in the transport of a basolateral protein. Both direct and indirect transport routes of apical proteins appear to be promoted by microtubules. Other mechanisms, such as vesicular recognition by the target membrane, may play an additional important role in sorting. Future work is needed to establish the precise way in which microtubules facilitate the targeting of plasma membrane proteins in epithelial cells.

Addendum

When this manuscript was ready for submission, a paper appeared by Matter et al. (43) having some similarities, but also considerable differences, with this report. Biotin targeting and transcytosis assays similar to ours were used to study the trafficking of APN, SI, and DPP and a different basolateral marker in Caco-2 cells treated with nocodazole instead of colchicine. Under the experimental conditions they used all apical markers became fully polarized in nocodazole-treated cells after the overnight chase whereas in our case no marker ever reached full polarity in the presence of colchicine, with some markers (ALP, DPP) remaining completely unpolarized after 20-h chase. We present here evidence that transcytotic rates may be considerably decreased by a cold preincubation step used in previous biotin transcytosis assays (36, 42, 43). The appearance of brush border in ectopic locations (basolateral membrane and intracellular vacuoles) in cells without microtubules was observed here, but not by Matter et al. (43). The differences between our results and those by Matter et al. may depend on different culture conditions (we use monolayers polarized for at least 2 wk) and different drugs used (colchicine vs. nocodazole, although we observe the appearance of intracellular vacuoles also in the presence of nocodazole). Finally, we describe here for the first time the three-dimensional microtubular organization of Caco-2 cells, using LSCM.

This work was supported by National Institutes of Health grants GM-34107 and HL-37675, a New York Heart Association grant-in-aid and a grant from the American Cancer Society. T. Gilbert was supported by a fellowship from L'Association pour la Recherche sur le Cancer (France) and A. Le Bivic by UA179 from Centre National de la Recherche Scientifique.

Received for publication 12 October 1990 and in revised form 18 December 1990.

References

1. Achler, C., D. Filmer, C. Merte, and D. Drenckhahn. 1989. Role of microtubules in polarized delivery of apical membrane proteins to be the brush border of the intestinal epithelium. *J. Cell Biol.* 109:179–189.
2. Allen, R. D., D. T. Brown, S. P. Gilbert, and H. Fujiwake. 1983. Transport of vesicles along filaments dissociated from squid axoplasm. *Biol. Bull. (Woods Hole).* 165:523–534.
3. Bacallao, R., C. Antony, C. Dotti, E. Karsenti, E. H. K. Stelzer, and K. Simons. 1989. The subcellular organization of Madin–Darby canine kidney cells during the formation of a polarized epithelium. *J. Cell Biol.* 109:2817–2832.
4. Bacallao, R., M. Bomsel, E. H. K. Stelzer, and J. DeMey. 1990. Guiding principles of specimen preservation for confocal fluorescence microscopy. *In* Handbook of Biological Confocal Microscopy. J. B. Pawley, editor. Plenum Publishing Co., New York. 197–205.
5. Bartles, J. R., H. M. Feracci, B. Stieger, and A. L. Hubbard. 1987. Biogenesis of the rat hepatocyte plasma membrane in vivo: comparison of the pathways taken by apical and basolateral proteins using subcellular fractionation. *J. Cell Biol.* 105:1241–1251.
6. Beaulieu, J. F., B. Nichols, and A. Quaroni. 1989. Posttranslational regulation of sucrase-isomaltase expression in intestinal crypt and villus cells. *J. Biol. Chem.* 264:20000–20011.
7. Bennett, M. K., A. Wandinger-Ness, and K. Simons. 1988. Release of putative exocytic transport vesicles from perforated MDCK cells. *EMBO (Eur. Mol. Biol. Organ.) J.* 13:4075–4085.
8. Blok, J., L. A. Ginsel, A. A. Mulder-Stapel, J. J. M. Onderwater, and W. T. Daems. 1981. The effect of colchicine on the intracellular transport of 3H-Fucose-labelled glycoproteins in the absorptive cells of cultured human small intestinal tissue. *Cell Tissue Res.* 215:1–12.
9. Bomsel, M., R. Parton, S. A. Kuznetsov, T. A. Schroer, and J. Gruenberg. 1990. Microtubule- and motor-dependent fusion in vitro between apical and basolateral endocytic vesicles from MDCK cells. *Cell.* 62:719–731.
10. Breitfeld, P. P., C. F. Simmons, G. J. A. M. Strous, H. J. Geuze, and A. L. Schwartz. 1985. Cell biology of the asialoglycoprotein receptor system: a model of receptor-mediated endocytosis. *Int. Rev. Cytol.* 97: 47–95.
11. Burgess, T. L., and R. B. Kelly. 1987. Constitutive and regulated secretion of proteins. *Annu. Rev. Cell Biol.* 3:243–293.
12. Caplan, M. J., B. Forbush, G. Palade, and J. Jamieson. 1990. Biosynthesis of the Na,K-ATPase in MDCK cells. *J. Biol. Chem.* 6:3528–3534.
13. Caplan, M. J., H. C. Anderson, G. E. Palade, and J. D. Jamieson. 1986. Intracellular sorting and polarized cell surface delivery of (Na^+,K^+) ATPase, an endogenous component of MDCK cell basolateral plasma membranes. *Cell.* 46:623–631.
14. Casanova, J. E., P. P. Breitfeld, S. A. Ross, and K. E. Mostov. 1990. Phosphorylation of the polymeric immunoglobulin receptor required for its efficient transcytosis. *Science (Wash. DC).* 248:742–745.
15. Chamberlain, J. P. 1979. Fluorographic detection of radioactivity in polyacrylamide gels with the water soluble fluor, sodium salicylate. *Anal. Biochem.* 98:132–135.
16. Cutz, E., M. Rhoads, B. Drumm, P. M. Sherman, P. R. Durie, and G. G. Forstner. 1989. Microvillus inclusion disease: an inherited defect of brush-border assembly and differentiation. *N. Engl. J. Med.* 320:646–651.
17. Danielsen, E. M., G. M. Cowell, and S. S. Poulsen. 1983. Biosynthesis of intestinal microvillar proteins. *Biochem. J.* 216:37–42.
18. Davidson, G. P., E. Cutz, J. R. Hamilton, and D. G. Gall. 1978. Familial enteropathy: a syndrome of protracted diarrhea from birth, failure to thrive, and hypoplastic villus atrophy. *Gastroenterology.* 75:783–790.
19. Drubin, D., S. Kobayashi, and M. Kirschner. 1986. Association of Tau protein with microtubules in living cells. *Ann. NY Acad. Med.* 466: 257–268.
20. Dustin, P. 1978. Microtubules. Springer Verlag, Berlin/Heidelberg, New York.
21. Eilers, U., J. Klumperman, and H. P. Hauri. 1989. Nocodazole, a microtubule-active drug, interferes with apical protein delivery in cultured intestinal epithelial cells (Caco-2). *J. Cell Biol.* 108:13–22.
22. Garland, D. L. 1978. Kinetics and mechanism of colchicine binding to tubulin: evidence for ligand-induced conformational change. *Biochemistry.* 17:4266–4272.
23. Deleted in proof.
24. Griffiths, G., and K. Simons. 1986. The trans-Golgi network: sorting at the exit site of the Golgi complex. *Science (Wash. DC).* 234:438–443.
25. Hagen, S. J., C. H. Allen, and J. S. Trier. 1987. Demonstration of microtubules in the terminal web of mature absorption cells from the small intestine of the rat. *Cell Tiss. Res.* 248:709–712.
26. Hauri, H. P., A. Quaroni, and J. Isselbacher. 1979. Biosynthesis of intestinal plasma membrane: posttranslational route and cleavage of sucrase-isomaltase. *Proc. Natl. Acad. Sci. USA.* 76:5183–5186.
27. Herman, B., and D. F. Albertini. 1984. A time-lapse video image intensification analysis of cytoplasmic organelle movements during endosome translocation. *J. Cell Biol.* 98:565–576.

28. Ho, W. C., V. J. Allan, G. van Meer, E. G. Berger, and T. E. Kreis. 1989. Reclustering of scattered Golgi elements occurs along microtubules. *Eur. J. Cell Biol.* 48:250–263.
29. Hugon, J. S., G. Bennett, P. Pothier, and Z. Ngoma. 1987. Loss of microtubules and alteration of glycoprotein migration in organ cultures of mouse intestine exposed to nocodazole or colchicine. *Cell Tiss. Res.* 248:653–662.
30. Kelly, R. B. 1990. Microtubules, membrane traffic, and cell organization. *Cell.* 61:5–7.
31. Laemmli, U. K. 1970. Cleavage of structural proteins during the assembly of the head of bacteriophage T4. *Nature (Lond.).* 227:680–685.
32. Langanger, G., J. De Mey, and H. Adam. 1983. 1,4-Diazobizyklo[2.2.2]oktan (DABCO) verzogest das ausbliechen von immunofluoreszenzpraparaten. *Mikroscopie.* 40:237–241.
33. Le Bivic, A., I. Bosc-Biern, and H. Reggio. 1988. Characterization of a glycoprotein expressed on the basolateral membrane of human intestinal epithelial cells and cultured colonic cell lines. *Eur. J. Cell Biol.* 46: 113–120.
34. Le Bivic, A., F. X. Real, and E. Rodriguez-Boulan. 1989. Vectorial targeting of apical and basolateral plasma membrane proteins in a human adenocarcinoma epithelial cell line. *Proc. Natl. Acad. Sci. USA.* 86:9313–9317.
35. Le Bivic, A., Y. Sambuy, K. Mostov, and E. Rodriguez-Boulan. 1990. Vectorial targeting of an endogenous apical membrane asialoglycoprotein and uvomorulin in MDCK cells. *J. Cell Biol.* 110:1533–1539.
36. Le Bivic, A., A. Quaroni, B. Nichols, and E. Rodriguez-Boulan. 1990. Biogenetic pathways of plasma membrane proteins in Caco-2, a human intestinal epithelial cell line. *J. Cell Biol.* 111:1351–1361.
37. Massey, D., H. Feracci, J. P. Gorvel, A. Rigal, J. M. Soulie, and S. Maroux. 1987. Evidence for the transit of aminopeptidase N through the basolateral membrane before it reaches the brush border of enterocytes. *J. Membr. Biol.* 96:19–25.
38. Lisanti, M., A. Le Bivic, M. Sargiacomo, and E. Rodriguez-Boulan. 1989. Steady-state distribution and biogenesis of endogenous Madin–Darby canine kidney glycoproteins: evidence for intracellular sorting and polarized cell surface delivery. *J. Cell Biol.* 109:2117–2127.
39. Lisanti, M., M. Sargiacomo, L. Graeve, A. Saltiel, and E. Rodriguez-Boulan. 1988. Polarized apical distribution of glycosyl phosphatidylinositol anchored proteins in a renal epithelial cell line. *Proc. Natl. Acad. Sci. USA.* 85:9557–9561.
40. Matlin, K. S., and K. Simons. 1984. Sorting of an apical plasma membrane glycoprotein occurs before it reaches the cell surface in cultured epithelial cells. *J. Cell Biol.* 99:2131–2139.
41. Matteoni, R., and T. E. Kreis. 1987. Translocation and clustering of endosomes and lysosomes depends on microtubules. *J. Cell Biol.* 105:1253–1265.
42. Matter, K., M. Brauchbar, K. Bucher, and H. P. Hauri. 1990. Sorting of endogenous plasma membrane proteins occurs from two sites in cultured human intestinal epithelial cells (Caco-2). *Cell.* 60:429–437.
43. Matter, K., K. Bucher, and H. P. Hauri. 1990. Microtubule perturbation retards both the direct and the indirect apical pathway but does not affect sorting of plasma membrane proteins in intestinal epithelial cells (Caco-2). *EMBO (Eur. Mol. Biol. Organ.) J.* 9:3163–3170.
44. Matter, K., B. Stieger, J. Klumperman, L. Ginsel, and H. P. Hauri. 1990. Endocytosis, recycling, and lysosomal delivery of brush border hydrolases in cultured human intestinal epithelial cells (Caco-2). *J. Biol. Chem.* 265:3503–3512.
45. Misek, D. E., E. Bard, and E. Rodriguez-Boulan. 1984. Biogenesis of epithelial cell polarity: intracellular sorting and vectorial exocytosis of an apical plasma membrane glycoprotein. *Cell.* 39:537–546.
46. Mostov, K. E., and D. L. Deitcher. 1986. Polymeric immunoglobulin receptor expressed in MDCK cells transcytoses IgA. *Cell.* 46:613–621.
47. Pavelka, M., and A. Ellinger. 1981. Effect of colchicine on the Golgi apparatus and on GERL of rat jejunal absorptive cells. Ultrastructural localization of thiamine pyrophosphatase and acid phosphatase activity. *Eur. J. Cell Biol.* 24:53–61.
48. Pavelka, M., A. Ellinger, and A. Gangl. 1983. Effect of colchicine on rat small intestinal absorptive cells. *J. Ultrastruct. Res.* 85:249–259.
49. Pinto, M., S. Robine-Leon, M. D. Appay, M. Kedinger, N. Triadou, E. Dussaulx, B. Lacroix, P. Simon-Assman, K. Haffen, J. Fogh, and A. Zweibaum. 1983. Enterocyte-like differentiation and polarization of the human colon carcinoma cell line Caco-2 in culture. *Biol. Cell.* 47:323–330.
50. Quaroni, A., and K. J. Isselbacher. 1985. Study of intestinal cell differentiation with monoclonal antibodies to intestinal cell surface components. *Dev. Biol.* 111:267–279.
51. Quaroni, A., K. Kirsch, and M. M. Weiser. 1979. Synthesis of membrane glycoproteins in rat small intestinal villus cells. *Biochem. J.* 182:213–221.
52. Rindler, M. J., I. E. Ivanov, H. Plesken, E. Rodriguez-Boulan, and D. D. Sabatini. 1984. Viral glycoproteins destined for apical or basolateral plasma membrane domains traverse the same Golgi apparatus during their intracellular transport in doubly infected Madin–Darby canine kidney cells. *J. Cell Biol.* 98:1304–1319.
53. Rindler, M. J., I. E. Ivanov, H. Plesken, and D. D. Sabatini. 1985. Polarized delivery of viral glycoproteins to the apical and basolateral plasma membranes of Madin–Darby canine kidney cells infected with temperature-sensitive viruses. *J. Cell Biol.* 100:136–151.
54. Rindler, M. J., I. E. Ivanov, and D. D. Sabatini. 1987. Microtubule-acting drugs lead to the nonpolarized delivery of the influenza hemagglutinin to the cell surface of polarized Madin–Darby canine kidney cells. *J. Cell Biol.* 104:231–241.
55. Rodriguez-Boulan, E., and W. J. Nelson. 1989. Morphogenesis of the polarized epithelial cell phenotype. *Science (Wash. DC).* 245:718–725.
56. Rodriguez-Boulan, E., K. T. Paskiet, P. J. Salas, and E. Bard. 1984. Intracellular transport of influenza virus hemagglutinin to the apical surface of Madin–Darby canine kidney cells. *J. Cell Biol.* 98:308–319.
57. Rodriguez-Boulan, E., and D. D. Sabatini. 1978. Asymmetric budding of viruses in epithelial monolayers: a model system for study of epithelial polarity. *Proc. Natl. Acad. Sci. USA.* 75:5071–5075.
58. Rodriguez-Boulan, E., and M. Pendergast. 1980. Polarized distribution of viral envelope proteins in the plasma membrane of infected epithelial cells. *Cell.* 20:45–54.
59. Salas, P. J., D. E. Misek, D. E. Vega Salas, D. Gundersen, M. Cereijido, and E. Rodriguez-Boulan. 1986. Microtubules and actin filaments are not critically involved in the biogenesis of epithelial cell surface polarity. *J. Cell Biol.* 102:1853–1867.
60. Sandoz, D., M. C. Laine, and G. Nicolas. 1985. Distribution of microtubules within the intestinal terminal web as revealed by quick-freezing and cryosubstitution. *Eur. J. Cell Biol.* 39:481–484.
61. Sargiacomo, M., M. Lisanti, L. Graeve, A. Le Bivic, and E. Rodriguez-Boulan. 1989. Integral and peripheral protein compositions of the apical and basolateral membrane domains in MDCK cells. *J. Membr. Biol.* 107:277–286.
62. Schwartz, A. L., S. E. Fridocich, and H. F. Lodish. 1982. Kinetics of internalization and recycling of the asialoglycoprotein receptor in a hepatoma cell line. *J. Biol. Chem.* 257:4230–4237.
63. Simons, K., and S. D. Fuller. 1985. Cell surface polarity in epithelia. *Annu. Rev. Cell Biol.* 1:243–288.
64. Solomon, F. 1986. Direct identification of microtubule-associated proteins by selective extraction of cultured cells. *Methods Enzymol.* 134:139–147.
65. Tucker, J. B., M. J. Milner, D. A. Currie, J. A. Muir, D. A. Forrest, and M. J. Spencer. 1986. Centrosomal microtubule organizing centers and a switch in the control of protofilament number for cell surface-associated microtubules during Drosophila wing morphogenesis. *Eur. J. Cell Biol.* 41:279–289.
66. Vale, R. D. 1987. Intracellular transport using microtubules-based motors. *Annu. Rev. Cell Biol.* 3:347–378.
67. Van DerSluijs, P., M. K. Bennett, C. Antony, K. Simons, and T. E. Kreis. 1990. Binding of exocytic vesicles from MDCK cells to microtubules in vitro. *J. Cell Sci.* 95:545–553.
68. Vega Salas, D. E., P. J. Salas, and E. Rodriguez-Boulan. 1987. Modulation of the expression of an apical plasma membrane protein of Madin–Darby canine kidney epithelial cells: cell–cell interactions control the appearance of a novel intracellular storage compartment. *J. Cell Biol.* 104: 1249–1259.
69. Wandinger-Ness, A., M. K. Bennett, C. Antony, and K. Simmons. 1990. Distinct transport vesicles mediate the delivery of plasma membrane proteins to the apical and basolateral domains of MDCK cells. *J. Cell Biol.* 111:987–1000.
70. Wilson, L., and K. W. Farrell. 1986. Kinetics and steady state dynamics of tubulin addition and loss at opposite microtubule ends: the mechanism of action of colchicine. *Ann. NY Acad. Sci.* 466:690–708.